

## Dimensional crossover in the magnetic phase diagram of $\text{Bi}_{2.15}\text{Sr}_{1.85}\text{CaCu}_2\text{O}_{8+\delta}$ crystals with different oxygen stoichiometry

C. M. Aegerter

*Physik-Institut der Universität Zürich, CH-8057 Zürich, Switzerland*

S. L. Lee

*School of Physics and Astronomy, University of St. Andrews, St. Andrews, Fife KY16 9SS, United Kingdom*

H. Keller

*Physik-Institut der Universität Zürich, CH-8057 Zürich, Switzerland*

E. M. Forgan and S. H. Lloyd

*School of Physics and Space Research, University of Birmingham, Birmingham B15 2TT, United Kingdom*

(Received 18 July 1996)

We have performed muon-spin-rotation measurements on the high-temperature superconductor  $\text{Bi}_{2.15}\text{Sr}_{1.85}\text{CaCu}_2\text{O}_{8+\delta}$  for a range of oxygen stoichiometries. The low-temperature in-plane penetration depth  $\lambda_{ab}$  was determined as a function of oxygen content. In addition, for each sample the crossover field  $B_{cr}$ , separating the regime of three-dimensional and quasi-two-dimensional vortex behavior, was measured. It is found that  $B_{cr}$  depends only on the penetration depth as  $B_{cr} = \Phi_0 / \lambda_{ab}^2$  rather than on the superconducting anisotropy  $\gamma$ . This may be understood in terms of a system of vortices controlled predominantly by electromagnetic interactions. The results are contrasted with other materials, such as  $\text{HgBa}_2\text{Ca}_3\text{Cu}_4\text{O}_{10+\delta}$ , where Josephson coupling plays a more significant role. [S0163-1829(96)50546-1]

High-temperature superconductors (HTSC's) are susceptible to both static (pinning induced) and dynamic (thermal) disorder. This is due to both the high transition temperatures and the anisotropic superconducting properties which arise from the layered structure of these compounds.<sup>1</sup> The anisotropic vortex behavior in HTSC's has been the subject of intense experimental (see, e.g., Refs. 2–7) and theoretical<sup>1,8–10</sup> investigations. In this work we address the dimensional crossover which occurs in the magnetic phase diagram of highly anisotropic HTSC's. In HTSC's the charge carriers are essentially confined to the  $\text{CuO}_2$  planes, so that they exhibit quasi-two-dimensional (2D) superconducting properties. In a field, a useful model of such a layered system consists of 2D pancake vortices, where the pancakes in neighboring planes interact via a combination of tunneling Josephson currents and electromagnetic interactions.<sup>11</sup> Depending on the strength of these interactions the pancakes form vortex-line-like objects with varying degrees of rigidity. The response of such vortex lines to dynamic and static disorder along their length depends strongly on the flux-line density. For fields greater than a characteristic field  $B_{cr}$  the energetic cost of an in-plane shear deformation begins to outweigh that for a tilt deformation to occur on the scale of the interlayer separation  $s$ , and the system thus adopts a more 2D character. Such a dimensional crossover for Josephson-coupled pancake vortices is usually expected to take place when the intervortex distance,  $a_0 = \sqrt{\Phi_0/B}$ , equals the Josephson length,  $\lambda_J = \gamma s$ ; here  $\Phi_0 = h/2e$  is the flux quantum and  $\gamma = \lambda_c / \lambda_{ab}$  is the superconducting anisotropy, where  $\lambda_c$  and  $\lambda_{ab}$  are the penetration depths for currents flowing perpendicular and parallel to the  $\text{CuO}_2$  planes,

respectively. This results in the prediction of a crossover field for the strongly Josephson-coupled case, which we shall call  $B_{2D} = \Phi_0 / (\gamma s)^2$ , which is fairly temperature independent for temperatures well below  $T_c$ . However, the relative strengths of the different interlayer coupling mechanisms (Josephson versus electromagnetic coupling) may radically affect the vortex behavior in the low-field region of the phase diagram,<sup>10</sup> and  $B_{cr}$  may no longer be equal to  $B_{2D}$ .

Due to its extremely high anisotropy,  $\text{Bi}_{2.15}\text{Sr}_{1.85}\text{CaCu}_2\text{O}_{8+\delta}$  (BSCCO) exhibits strong quasi-2D behavior and therefore has attracted much interest. Of particular value are those experimental methods which microscopically probe the vortex state, such as small-angle neutron scattering (SANS), nuclear magnetic resonance (NMR), and muon-spin rotation ( $\mu\text{SR}$ ). These have been crucial for understanding the nature of the unconventional phenomena observed in HTSC's, such as vortex lattice melting and decoupling.<sup>4–6</sup> We have recently shown by means of  $\mu\text{SR}$  that in BSCCO at low temperatures the in-plane penetration depth is smaller than the Josephson length  $\lambda_{ab} < \lambda_J$ , and the dominant coupling mechanism between the pancake vortices is of electromagnetic origin over large regions of the phase diagram.<sup>2</sup> As a consequence the experimental determination of  $\gamma$  is very difficult, because it cannot be inferred from measurements of the melting line or from angular-dependent magnetization measurements.<sup>10</sup> This dominance of the electromagnetic coupling also suggests that in general  $\gamma$  should play a reduced role in determining the phase diagram.<sup>10</sup> A dimensional crossover in BSCCO has been observed by  $\mu\text{SR}$  (Ref. 4) and SANS,<sup>5</sup> where it is apparent via the increased effects of thermal and pinning disorder on the vortex

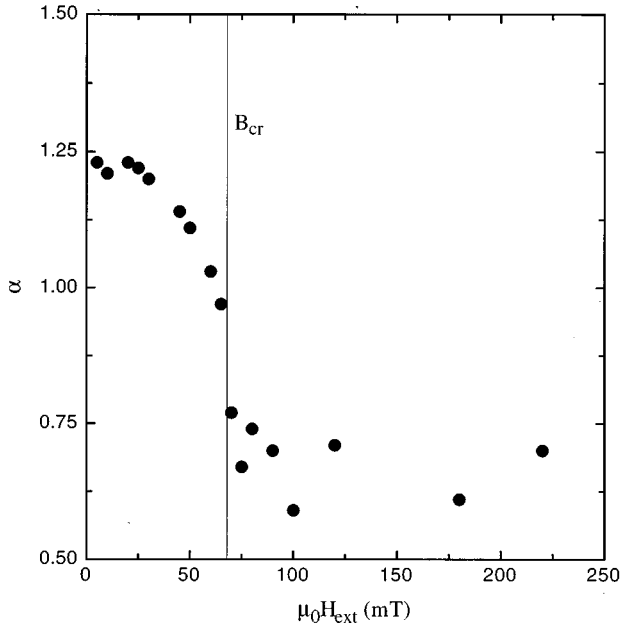


FIG. 1. The skewness parameter  $\alpha = \langle \Delta B^3 \rangle^{1/3} / \langle \Delta B^2 \rangle^{1/2}$  of the  $\mu$ SR line shape as a function of the applied field  $H_{\text{ext}}$ , for the overdoped BSCCO sample  $S_2$  after cooling at each field to a temperature of 5 K. The line shape and corresponding  $\alpha$  observed below the crossover field  $B_{\text{cr}}$  are characteristic of a vortex-line lattice (see text). Increasing  $c$ -axis disorder above  $B_{\text{cr}}$  results in a symmetric  $\mu$ SR line shape, displayed by a decrease in  $\alpha$  at the crossover field  $B_{\text{cr}}$ .

lattice. At low temperatures and for fields higher than a characteristic crossover field  $B_{\text{cr}}$ , the enhanced susceptibility to tilt deformations allows pinning sites to distort the vortex lines in the lattice into a state which is highly disordered along crystallographic  $c$  axis and which is more reminiscent of a vortex glass than a vortex lattice. This crossover in BSCCO may also be detected via measurements of magnetization versus the applied field. The hysteresis loops typically obtained are very different from those of a conventional superconductor. They exhibit a characteristic double-peak structure, which has been attributed to a variety of causes such as surface barrier effects,<sup>12</sup> a crossover from surface to bulk pinning,<sup>13</sup> sample inhomogeneities,<sup>14</sup> and a 3D to 2D transition.<sup>15</sup> It has been the microscopic methods of  $\mu$ SR and SANS, in combination with magnetization measurements, which have led to an improved understanding of this effect. Such measurements show good agreement between the appearance of the so called “second peak” at a field  $H_p$  in  $M(H)$  loops, and a sharp change in the microscopic field distribution at the same field (see Fig. 1).<sup>16,17</sup> This change in the field probability distribution is associated with an increase in  $c$ -axis disorder above the crossover field  $B_{\text{cr}}$ , clearly indicating a dimensional crossover.<sup>4</sup> While it is the influence of point pinning centers on the vortices which permits an observable change in both the  $\mu$ SR and magnetization measurements, the sharpness of the crossover in field suggests an underlying mechanism. Recent experiments to examine the influence of increased random pinning on  $B_{\text{cr}}$ , by irradiating BSCCO samples with high doses of 2.5 MeV electrons, produced only an approximately 10% decrease in

$B_{\text{cr}}$ .<sup>18</sup> However, much more significant shifts of  $B_{\text{cr}}$  are possible via oxygen doping. We have performed a systematic study of BSCCO as a function of oxygen stoichiometry, which is known to influence many of the superconducting properties such as  $\gamma$  and  $\lambda_{ab}$ . This has allowed us to demonstrate the very different properties of a vortex system where electromagnetic coupling dominates the vortex behavior. In particular, we have been able to identify clearly a relationship between the crossover field  $B_{\text{cr}}$  and the penetration depth  $\lambda_{ab}$ , which is the main result of this work.

The samples were grown using a floating zone technique described elsewhere<sup>19</sup> and then oxygen treated to give different anisotropies  $\gamma$  and low-temperature penetration depths  $\lambda_{ab}(0)$ . The experiments were performed on beamline  $\pi$ M3 at the Paul Scherrer Institute, Switzerland and at the ISIS MUSR facility at the Rutherford Appleton Laboratory, UK, using experimental setups as described in Refs. 3 and 4. In a  $\mu$ SR experiment the spin-polarized muons precess in the local internal field of the mixed state of the superconductor. From the distribution of these precession frequencies the field probability distribution  $p(B)$  can be determined. For a lattice structure consisting of straight vortex lines (3D vortex lattice)  $p(B)$  is expected to show a long tail at high fields (higher than the applied field) due to muons stopping in the vicinity of a vortex-line core. The field distribution for a 3D lattice is therefore expected to be weighted towards fields higher than the average, resulting in a positive skewness of  $p(B)$ . One way to quantify the skewness of the distribution is by the ratio of the third and the second moments  $\alpha = \langle \Delta B^3 \rangle^{1/3} / \langle \Delta B^2 \rangle^{1/2}$ . Numerical simulations of our experiments predict a value of  $\alpha = 1.2$  for a 3D vortex lattice, measured under the conditions of the experiment.<sup>4</sup> Assuming a constant in-plane order in the lattice, for  $B > B_{\text{cr}}$  the increasing  $c$ -axis disorder, due to pinning and thermally induced vortex fluctuations, leads to a truncation of the high-field tail<sup>20</sup> and therefore to a narrowed and more symmetric line shape. This has been shown experimentally to occur as  $\alpha \rightarrow \sim 0.5$ . These arguments are also discussed in Refs. 4 and 17 and lead to an identification of the crossover field from  $\mu$ SR with a drop in  $\alpha$ , as shown in Fig. 1. The observation of the crossover field is also possible from SANS experiments and is indicated by the loss of scattered neutron intensity due to the loss of short-range  $c$ -axis order.<sup>5</sup>

The  $\mu$ SR technique allows a determination of the superconducting penetration depth  $\lambda_{ab}$  from the measured line shapes. The most commonly used method to extract  $\lambda_{ab}$  is via the linewidth  $\langle \Delta B^2 \rangle \propto \lambda_{ab}^{-4}$ . This is in fact not the most reliable approach for single crystals that exhibit line shapes arising from an almost ideal vortex-line lattice. In this case the long high-field tails, arising from fields close to the vortex cores, are often underestimated due to their low probability density  $p(B)$ , which is of the order of the spectral noise for realistically achievable experimental statistics. This often leads to a significant underestimate of the linewidth  $\langle \Delta B^2 \rangle$  and thus to an overestimate of  $\lambda_{ab}$ . A more reliable method is to use the separation of the mode  $B_{\text{sad}}$  and mean  $\langle B \rangle$  of the probability distribution  $p(B)$ . This gives<sup>21</sup>

$$\langle B \rangle - B_{\text{sad}} = \ln 2 \frac{2}{3} \frac{\Phi_0}{4\pi\lambda_{ab}^2}. \quad (1)$$

TABLE I. The experimentally determined penetration depth  $\lambda_{ab}$  and the crossover field  $B_{cr}$  for the samples studied in this and other works. Also given is the calculated crossover field  $\Phi_0/\lambda_{ab}^2$ . The fields are given in mT. For the BSCCO and TI-2212, with  $\lambda_{ab} < \gamma s$ , these values agree well with the experimentally determined  $B_{cr}$ . For these samples we estimate the lower bound for  $\gamma$  by taking  $B_{cr}$  as an upper bound for  $B_{2D}$  (see text). The value for the anisotropy given for the Hg-1234 sample is measured by means of high-precision torque magnetometry (Ref. 23). Note that for this Hg-1234 sample ( $s = 1.5$  nm)  $\lambda_{ab} > \gamma s$ , and that the experimental crossover is better described by the conventional relation  $B_{2D} = \Phi_0/(\gamma s)^2$  rather than by  $\Phi_0/\lambda_{ab}^2$  as expected.

sample	$\lambda_{ab}$ (nm)	$B_{cr}^{exp}$	$\Phi_0/\lambda_{ab}^2$	$\gamma$
BSCCO $S_1^a$	270(10)	29(2)	28(2)	$>180$
BSCCO $S_2^a$	180(10)	67(2)	64(5)	170 <sup>f</sup>
BSCCO $S_3^a$	260(10)	32(3)	31(2)	$>175$
BSCCO <sup>b</sup>	180	64(2)	64	$>120$
BSCCO <sup>b</sup>	240	38(2)	36	$>160$
BSCCO <sup>b</sup>	260	27(2)	30	$>175$
TI-2212 <sup>c</sup>	200	54(3)	52	$>135$
Hg-1234	130(20) <sup>d</sup>	230(15) <sup>e</sup>	122(20)	52.6(5) <sup>d</sup>

<sup>a</sup>This work.

<sup>b</sup>Reference 7.

<sup>c</sup>Reference 12.

<sup>d</sup>Reference 23.

<sup>e</sup>Reference 22.

<sup>f</sup>Reference 2.

$B_{sad}$  and  $\langle B \rangle$  may be determined from the measured spectra  $p(B)$  with a much reduced systematic error compared to  $\langle \Delta B^2 \rangle$ , and  $\langle B \rangle$  may also be checked independently via magnetization measurements from  $\langle B \rangle = \mu_0[H_{app} + (1-n)M]$ , where  $H_{app}$  is the applied field,  $M$  the magnetization and  $n$  the demagnetization factor.

We have performed experiments on an as-grown single crystal  $S_1$ , on a slightly over-doped single crystal  $S_2$  and on a mosaic of nearly optimally doped single crystals  $S_3$ . For each of these samples we determined the crossover field  $B_{cr}$  by measuring the field-cooled  $\mu$ SR line shape as a function of applied field. The crossover is clearly apparent as a marked narrowing of the linewidth  $\langle \Delta B^2 \rangle$  at  $B_{cr}$ , or as a simultaneous reduction in the skewness of the line shape  $\alpha$ , as shown in Fig. 1. From data taken at  $B < B_{cr}$  we have also determined  $\lambda_{ab}(0)$  for each of the samples  $S_1, S_2, S_3$  using Eq. (1). The results are summarized in Table I. For comparison we have also included other measurements on BSCCO taken from Ref. 7, and on the similarly anisotropic compound  $Tl_2Sr_2Ca_1Cu_2O_{8+\delta}$  (TI-2212) from Ref. 12. These measurements use the observation of the second peak  $H_p$  in magnetization measurements as an indication of the crossover field  $B_{cr}$ . In Fig. 2 the experimental values of the crossover field  $B_{cr}$  are plotted as a function of  $\lambda_{ab}^{-2}(0)$ . The proportionality between the two quantities is obvious. Moreover, the slope of the straight line is equal to the flux quantum  $\Phi_0$ , showing that  $B_{cr} = \Phi_0/\lambda_{ab}^2(0)$ . This result is at first rather surprising, since for a Josephson-coupled system one would expect that the crossover should occur at  $B_{2D} = \Phi_0/(\gamma s)^2$ . However, as we shall discuss below, this result is not totally unexpected given that BSCCO and TI-

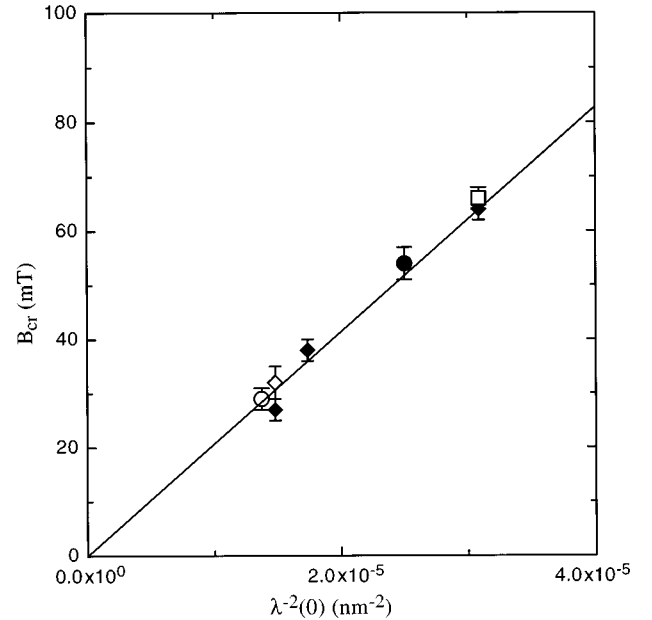


FIG. 2. The crossover field  $B_{cr}$  as a function of  $\lambda_{ab}^{-2}(0)$  for different samples. Open symbols correspond to  $\mu$ SR measurements on samples studied in this work: circle:  $S_1$ ; square:  $S_2$ ; diamond:  $S_3$ . Filled diamonds are taken from Ref. 7 and are obtained from magnetization measurements using Hall bar arrays. Filled circles are from a TI-2212 sample taken from Ref. 12, where the crossover field is determined by magnetization measurements. The solid line corresponds to the relation  $B_{cr} = \Phi_0/\lambda_{ab}^2$  which describes the data without any adjustable parameter. These data are summarized in Table I, also including additional data on the Hg-1234 compounds, not shown in this plot (see text).

2212 are dominated by electromagnetic interactions. We have not included data from Ref. 17 in which  $B_{cr}$  was determined both by  $\mu$ SR and magnetization measurements in Fig. 2 and in Table I. This is because in that paper  $\lambda_{ab}$  is estimated from the  $\mu$ SR linewidth, which systematically overestimates the value of the penetration depth as described above. Due to the complexity of the magnetic phase diagram of BSCCO, it is difficult to perform a more appropriate analysis of their line shape without access to a more complete data set than that given in Ref. 17. However, we note that the range of values of  $\langle B \rangle - B_{sad} \propto \lambda_{ab}^{-2}$  in their work is consistent with the range of  $B_{cr}$  they measure. In Table I, we have also included recent results on a ‘‘second peak’’ in  $M(H)$  loops taken on single crystal  $HgBa_2Ca_3Cu_4O_{10+\delta}$  (Hg-1234) using the technique of high-precision torque magnetometry.<sup>22</sup> For this Hg-1234 sample the anisotropy and penetration depth were measured in angular-dependent torque measurements, yielding  $\gamma = 52.6(5)$  and  $\lambda_{ab} = 130(20)$  nm.<sup>23</sup> Thus in contrast to the other samples studied, for this sample  $\lambda_{ab}(0) > \gamma s = 80(20)$  nm, which is the condition for Josephson coupling to dominate over electromagnetic coupling.<sup>10</sup> Furthermore, this material fails to obey the relation  $B_{cr} = \Phi_0/\lambda_{ab}^2(0)$ , and in fact is much better described by  $B_{2D} = \Phi_0/(\gamma s)^2 = 280(60)$  mT, in fair agreement with the measured crossover field of 230(15) mT. For all of the other samples investigated the condition  $\lambda_{ab} < \gamma s$  holds, implying the dominance of electromagnetic coupling

and the crossover field is found experimentally to obey  $B_{\text{cr}} = \Phi_0 / \lambda_{ab}^2(0)$ . Since in this case [ $\lambda_{ab}(0) < \gamma s$ ] it always follows that  $B_{\text{cr}} > B_{2\text{D}}$ , and  $B_{\text{cr}}$  may thus be taken as an upper estimate of  $B_{2\text{D}}$  and hence can be used to provide a lower limit for  $\gamma$ . These values have also been included in Table I. The previously published values of  $\gamma$  from Ref. 17 should thus be regarded as lower bounds for the true anisotropy. It has recently been shown theoretically<sup>10</sup> and experimentally,<sup>2</sup> that for  $\lambda_{ab}(0) < \gamma s$  the dominant role of electromagnetic coupling implies that over most of the phase diagram the melting or decoupling line does not depend on  $\gamma$ . Thus attempts to extract the value of  $\gamma$  in this way may provide an even worse estimate.<sup>3,7</sup> The value of  $\gamma$  is only important in the description of the high-temperature region of the phase diagram, and in BSCCO  $\gamma$  can be inferred from the melting line only above the characteristic temperature  $T^{\text{em}}$ .<sup>10</sup> For sample S<sub>2</sub> it has been shown recently<sup>2</sup> that  $T^{\text{em}} \approx 70$  K. From this characteristic temperature  $\gamma$  was estimated to be  $\sim 170$  for that sample. This value has also been included in Table I. We note that the value for  $B_{2\text{D}} \sim 30$  mT resulting from such a  $\gamma$  coincides with the apparent roll off of  $\alpha$  visible in Fig. 1.

For a vortex system dominated by electromagnetic interactions at low temperature,  $\lambda_{ab} < \gamma s$ , and the field  $B_{2\text{D}} = \Phi_0 / (\gamma s)^2 < B_{\text{cr}} = \Phi_0 / \lambda_{ab}^2(0)$ . In general the energetic cost of shear deformations of the lattice should increase relative to tilt deformations for  $B > B_{2\text{D}}$ . However, for the situation  $\lambda_{ab}(0) < \gamma s$  the flux-lines are only weakly interacting within the planes at  $B_{2\text{D}}$ , since the lattice parameter  $a_0 = \gamma s \gg \lambda_{ab}$  and hence the vortices are still dilute. A more significant effect occurs as  $a_0$  decreases below  $\lambda_{ab}$  for fields  $B > B_{\text{cr}}$ . It

is then that the vortices begin to overlap strongly and there is a crossover from an exponential to a linear field dependence in the shear modulus  $c_{66}$  of the system.<sup>10</sup> It might then be expected that short wavelength tilt deformations of the lattice would become increasingly more likely, leading to a more quasi-2D behavior. Thus for  $B > B_{\text{cr}}$  the vortices are more susceptible to disorder along the field axis, which can arise from either pinning or thermally induced fluctuations of the vortices about their average position.

In conclusion, we have shown that for a range of BSCCO samples the anisotropy is sufficiently large that the pancake interactions are largely dominated by electromagnetic rather than Josephson coupling ( $\lambda_{ab} < \gamma s$ ). This is revealed by means of the crossover field  $B_{\text{cr}}$ , which obeys  $B_{\text{cr}} = \Phi_0 / \lambda_{ab}^2$  rather than  $B_{\text{cr}} = B_{2\text{D}} = \Phi_0 / (\gamma s)^2$ . This is also observed in the TI-2212 sample which has a similar anisotropy to BSCCO. For the less anisotropic Hg-1234 compound, with  $\lambda_{ab}(0) > \gamma s$ , the more conventional expression for the crossover field  $B_{2\text{D}} = \Phi_0 / (\gamma s)^2$  appears to be satisfied. The observed behavior of anisotropic layered superconductors with dominant electromagnetic coupling may be qualitatively explained as arising from the crossover in the ratio of the shear modulus  $c_{66}$  to the tilt modulus  $c_{44}$ , which occurs as  $B$  increases above  $B_{\text{cr}}$ , where the vortices begin to overlap strongly.

We would like to thank T. W. Li for the preparation of the samples, the staff at Paul Scherrer Institute and Rutherford Appleton Laboratory for technical assistance as well as M. B. Hunt and Guo-meng Zhao for helpful discussions. This work was supported by the Swiss National Science Foundation and by the EPSRC of the United Kingdom.

<sup>1</sup>M. P. A. Fisher, D. S. Fisher, and D. A. Huse, *Phys. Rev. B* **43**, 130 (1991).  
<sup>2</sup>S. L. Lee *et al.*, *Phys. Rev. Lett.* (unpublished).  
<sup>3</sup>S. L. Lee *et al.*, *Phys. Rev. Lett.* **75**, 922 (1995).  
<sup>4</sup>S. L. Lee *et al.*, *Phys. Rev. Lett.* **71**, 3862 (1993).  
<sup>5</sup>R. Cubitt *et al.*, *Nature* **365**, 407 (1993).  
<sup>6</sup>Y.-Q. Song *et al.*, *Phys. Rev. Lett.* **70**, 3127 (1993).  
<sup>7</sup>B. Khaykovich *et al.*, *Phys. Rev. Lett.* **76**, 2555 (1996).  
<sup>8</sup>L. I. Glazman and A. E. Koshelev, *Phys. Rev. B* **43**, 2835 (1991).  
<sup>9</sup>G. Blatter *et al.*, *Rev. Mod. Phys.* **66**, 1125 (1994).  
<sup>10</sup>G. Blatter *et al.*, *Phys. Rev. B* **54**, 72 (1996).  
<sup>11</sup>W. E. Lawrence and S. Doniach, in *Proceedings of the Twelfth International Conference on Low Temperature Physics, Kyoto, 1970*, edited by E. Kanda (Keigaku, Tokyo, 1971), p. 361.

<sup>12</sup>V. N. Kopylov *et al.*, *Physica C* **170**, 291 (1990).  
<sup>13</sup>N. Chikumoto *et al.*, *Phys. Rev. Lett.* **69**, 1260 (1992).  
<sup>14</sup>M. Daeumling *et al.*, *Nature* **346**, 332 (1990).  
<sup>15</sup>G. Yang *et al.*, *Phys. Rev. B* **48**, 4054 (1993).  
<sup>16</sup>E. M. Forgan *et al.*, in *Proceedings of the 7th International Workshop on Critical Currents in Superconductors, Alpbach, 1994*, edited by H. W. Weber (World Scientific, Singapore, 1994), p. 264.  
<sup>17</sup>C. Bernhard *et al.*, *Phys. Rev. B* **52**, R7050 (1995).  
<sup>18</sup>B. Khaykovich *et al.* (unpublished).  
<sup>19</sup>T. W. Li *et al.*, *J. Cryst. Growth* **135**, 481 (1994).  
<sup>20</sup>E. H. Brandt, *Phys. Rev. Lett.* **66**, 3213 (1991).  
<sup>21</sup>A. D. Sidorenko *et al.*, *Hyperfine Interact.* **63**, 49 (1990).  
<sup>22</sup>J. Hofer and C. M. Aegerter (unpublished).  
<sup>23</sup>D. Zech *et al.*, *Phys. Rev. B* **53**, R6026 (1996).